Peer-reviewed version available at *Minerals* **2020**, *10*, 321; doi:10.3390/min10040321

Article

Mineralogical Characterization of Slags from Oiola Site (Biscay) to Assess the Development in Bloomery Iron Smelting Technology from the Roman Period to the Early Middle Ages

Haizea Portillo-Blanco [1], Maria Cruz Zuluaga [1*], Luis Angel Ortega [1], Ainhoa Alonso-Olazabal [1], Juanjo Cepeda-Ocampo [2] and Ana Martínez Salcedo [3]

[1] *University of the Basque Country, Dept. of Mineralogy and Petrology, P.O. Box 644, E-48080 Bilbao, Spain; haizea.portillo@ehu.eus; mcruz.zuluaga@ehu.eus; luis.ortega@ehu.eus; ainhoa.alonso@ehu.eus.*

[2] *48080 University of Cantabria, Historical Sciences, 39005 Santander, Spain; juanjcepeda@outlook.es.*

[3] *ARKEON, Plaza Julio Lazurtegui, 6 4º dcha. 48014-Bilbao, Spain; arkeon@euskalnet.net.*

Abstract: Oiola archeological site, located in the mining complex of La Arboleda (Biscay, North Spain) was an important iron smelting center from the Roman Period to the Early Middle Ages and even in more current times (19th-20th centuries). Tap-slags and some plano-convex slags were identified as smelting slags. Samples were analyzed by optical microscopy, X-ray powder diffraction, scanning electron microscopy coupled with electron-dispersive spectroscopy and Raman microspectroscopy to perform a mineralogical and textural characterization. Additionally, thermogravimetric and thermodiffraction analyses were carried out to determine furnace operating temperatures. The mineral assemblage reflects furnace cooling rates and temperatures and the addition of quartz as the main flux to decrease the melting temperature of the iron ore. The comparison of slags from the Roman Period and the Early Middle Age allows to observe changes in the pyrometallurgical process through time.

Keywords: smelting slags; multianalytical study; furnace operating conditions; Roman Period; Early Middle Age; North Spain

1. Introduction

In ancient times, from the Iron Age to the appearance of blast furnaces and cast iron in the Middle Ages (10th century BC - 20th century AD), iron was obtained by the direct solid-phase reduction method, also called "bloomery" method and a posterior smithing (forging) process. In the bloomery process, the iron oxides from the ore are processed, in one step, in a furnace with carbon-based fuel and reducing agent (usually charcoal) at temperatures of about 1200 °C [1-6]. Inside the furnace, carbon monoxide (CO) gas emanating from the charcoal reacts with iron oxide (FeO) in the ore to form solid iron particles and carbon dioxide (CO_2) gas [7]. Additionally, to reach the high temperatures needed, bellows were used to blow air into the furnace through one or more blowing holes in the side. Sometimes ceramic tubes, known as tuyères, may have been inserted into the furnace to direct air inside [7]. Fluxes can also be added deliberately to promote greater yields of iron and lower melting temperatures [6]. Flux elements consist of minerals such as lime and quartz rich sands or sandstones [2,7,8].

The metallic product, called bloom, is a heterogeneous spongy mass, more or less consolidated and with a large number of pores. The reduction of the metals starts at temperatures of around 800 °C but metal never reaches its molten condition (as high as 1540 °C) and remains solid [2,5,9-12].

Peer-reviewed version available at Minerals 2020, 10, 321; doi:10.3390/min10040321

The other substances present in the load inside the furnace, mainly silica, alumina and unreduced iron oxides, are thermochemically removed as a liquid phase that separates and flows away from the metal in an iron smelting slag [2,6]. Some of these impurities can also be driven off as a gas, alloy with the iron or even stay inside the furnace [13]. The solid iron bloom, even if it is much denser than the slag, does not sink to the base of the furnace. It attaches to the furnace wall just below the tuyère level [14].

The slags are essentially the main by-product of the iron production process. The composition of smelting slags depends on the furnace operation (design, air supply mechanism), raw material used (ore, charcoal, furnace lining) and potential use of a flux [10,15-17]. Additionally, slags might contain constituents formed from the reaction with other impurities in the ore or molten material from the technical ceramics such as tuyères [10,16,17]. Therefore, smelting slags have a composition near that of fayalite (Fe_2SiO_4) formed by the reaction at high temperatures (1200 °C) between the iron oxide and silica added in the form of sand, resulting in a molten ferrosilicate slag. They contain both fayalite crystals and residual glass of similar composition, sometimes with a fine fayalite precipitate. When iron oxide is in excess, dendrites of wuestite and/or magnetite also precipitate. In addition to silicates and oxides, iron slags almost invariably contain droplets of metallic iron [18,19]. The production of this slag reduces the amount of FeO available for reduction and provides a fluid medium through which metallic particles are transported, fused into larger masses, and protected from re-oxidation [7].

On the basis of textural, mineralogical and chemical features, iron smelting slags can be further subdivided into different groups. Even so, the characteristic representatives of slags from the bloomery processes are tap-slags. Tap-slags are usually very heavy, compact with an absence of blowholes and completely melted homogeneous pieces. They have a shiny black surface with cord-like flows or flat slab structures when tapped and cooled outside the furnace and a flat base. Minor gas bubbles can be found in their dark-grey fractures [19,20]. These morphologies are due to the "tapping furnaces", known from the late Iron Age, Roman and Medieval periods, used for the iron smelting process. Tapping furnaces have a hole in the furnace wall at ground level that could be opened during the smelt and from where the slag could run out.

In other cases, slags are trapped at the base of the furnace in a previously excavated pit with a large cylindrical shape. This group is the so-called cinder. Cinder slags are large, strongly indented, sponge-like slag-blocks and with a lot of blowholes. They have a less dense and more heterogeneous structure than that of tap-slags. Sometimes calcareous and charcoal gathering-up inclusions can appear [2,20]. At the same time, there are some pieces of slag of a special kind of transition type which combine the properties of both groups. These transition slags are entirely melted and compact pieces and their morphology is closer to the morphology of the cinder. Often these slags have a plano-convex shape [20].

The texture of the slag, vitreous or crystallized, is related to both the chemistry and the cooling conditions [2]. Slag chemistry, instead, depends on the furnace temperature, redox conditions, reaction speed, and the chemical constraints imposed by the raw and flux materials [1,6,7]. All of these materials, even if their source is the same, are heterogeneous and compositionally variable. Consequently, processing of the raw materials and the conditions within the furnace would influence the composition of the slag [17].

The air supply mechanism and the fuel to ore ratio can be the most important features providing the high temperature and a reducing atmosphere in the furnace. These conditions are necessary to reduce the iron minerals in the ore into a single mass and maintain a fluid slag, with sufficiently low viscosity to separate from the bloom being produced [7,17]. Conversely, if the conditions within the furnace are not reducing enough, an iron-rich fluid slag is formed but no metal is produced [21]. Nevertheless, for the production of metallic iron, a considerable amount of ferric oxide must be sacrificed to produce slag, making bloomery smelting a fairly inefficient process [15].

The largest available and most accessible data set for investigating old iron production technologies is slag. The study of textural and mineralogical features of slags can give information about bloomery smelting techniques and conditions even when other forms of evidence are missing.

The aim of this work is to determine the compositional and structural affinities or differences of Roman and Early Middle Age slags from the archaeological site of Oiola (Bizkaia, Spain) in order to establish the development of iron-making processes and technologies through time. Since slag composition and structure are closely related to the materials used and the conditions of slag formation, the combination of resource usage, furnace design, air supply mechanism, fuel type or operating procedures and conditions can be determined.

2. Geological context

The iron ore corresponds to the largest proportion of the slag composition. The specific localization of the ore, as well as the raw materials, and fuel, implies moving to these points where the operative chain starts [8,17]. The archaeological site of Oiola corresponds to the municipality of Trapagarán (Bizkaia) while it borders at its S-SW end with Galdames (Fig. 1). This area is near the mining complex of La Arboleda from where different iron ores were exploited from Roman times until the 20th century.

During Roman times and the Early Middle Ages (until the 19th century), iron ores used in Oiola for iron reduction correspond mainly to ores that are dominated by quartz components (SiO_2) and a limonite matrix [22]. Limonite is a generic term for amorphous and crystalline iron-hydroxides and iron-oxides in varying compositions, mainly yellow-brownish goethite (α-FeO(OH)) formed under oxidizing conditions [23,24]. Hematite (α-Fe_2O_3) has also been observed as representative of Fe oxides [24]. This type of ore is called "bog iron ore" or "bog ore".

The mineralogical composition of a bog iron ore layer can be divided into a ferric upper horizon with oxidizing conditions and a ferrous lower horizon with reducing conditions [25]. The lower horizon tends to contain siderite ($FeCO_3$), whereas in the top horizon the hematite ($Fe^{3+}{}_2O_3$) and goethite ($Fe^{3+}O(OH)$) mineral phases prevail, formed due to the supergenic alteration of the siderite [24].

The composition of the ore and the prevailing iron-oxides and iron–hydroxide phases depend on the elemental composition of the parent sediment in terms of geologic formations, the hydrological situation of the study area and the composition of groundwater fluxes, which work as a source of iron [26].

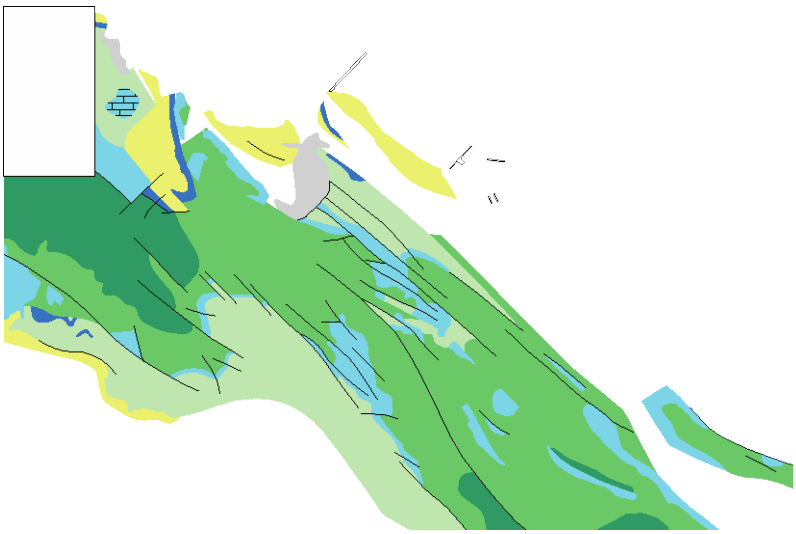

Figure 1. Geographical and geological location of Oiola archaeological site; (**b**) scheme of the type of mineralization the iron oxyhydroxides.

According to the geology of the study area, Oiola and the area of La Arboleda are located on the northern flank of the Bilbao anticline where Lower Cretaceous materials prevail, mainly of Aptian (~125-113 Ma) and Albian (~113-100.5 Ma) age. The Aptian-Albian series is represented by Urgonian

Peer-reviewed version available at Minerals 2020, 10, 321; doi:10.3390/min10040321

and Supra-Urgonian limestones, and sits above a Barremian series formed by the alternation of sandstones and black marls [27] (Fig. 1).

Urgonian limestones, of Aptian age, have been of great importance in mining, since were formed when the opening of the Bay of Biscay (Rift type) took place. As a result of this the earth's crust fractured and through these fractures came fluids enriched with elements such as iron. These fluids, when mixed with the carbonate that was being deposited at that time, created siderite primary deposits. The siderite that comes to the surface due to the uplifting and erosion of the overlying sediments is altered and oxidized in supergenic conditions (oxidation of Fe^{2+} to Fe^{3+}). Therefore, hematite and goethite iron-oxide and iron–hydroxides are formed as secondary mineralization. This type of accumulation of iron-oxides and iron-hydroxides mixed with clays and quartz of very fine grain size is known locally as "Txirteras" [28] (Fig. 1b).

The final product of the alteration processes is conditioned by the relative proportion of oxygen and water. In oxygenated environments Fe^{3+} is combined as oxide (hematite), while in the case of excess water, Fe^{3+} stabilizes as hydroxide (goethite) [28]. These secondary mineralizations have a higher concentration of iron than siderite. Moreover, the extraction of iron from this mineral is easier and of better quality. Weathering is beneficial, as the resulting ore is more iron-rich than the original deposit due to the dissolution of many of the gangue minerals [29]. The iron content of these minerals can reach 60-70%.

Currently, due to the transformation of the landscape and the remodeling of the old dumps, there are few testimonies of this type of mineralization. The oxidation zones corresponding to this mineralization have been exploited until exhaustion [28,30].

The extracted hematite and goethite ores had to be processed before smelting. Ores were first washed and sorted to enrich their iron content and reduce the amount of unwanted material, which would influence the resulting slag composition. Afterwards ores were roasted to make them more porous and reducible, and smashed into preferred size ranges. At a single site, ores from a variety of sources could have been smelted, either in different smelts or blended together in the same smelt [7,17].

3. Archaeological background

The metallurgical workshop of Oiola is one of the very few sites belonging to the Roman and medieval periods in the Basque Country. This site has revealed a set of organized structures corresponding to the stage of iron reduction or smelting process during different periods of occupation: from the Late Roman Period (4th century AD) to the Early Middle Ages (from the 5th or 6th centuries to the 10th century). However, no archaeological work has confirmed that the occupation during this period was continuous. For economy reasons, direct reduction furnaces are near the extraction and supply site. Accordingly, slag remains from the reduction phase have been found in the archaeological site of Oiola.

In 1989, three zones were chosen to be surveyed. These areas were called OIOLA I, II and III. At the end of this first season a new zone was chosen, which was designated as OIOLA IV. Of the four surveyed areas, I and III were sterile and of little archaeological interest respectively, and research focused on Zones II and IV. Between 1991 and 1992 the excavation was continued in these two zones [31].

The oldest archaeological settlement finds in this area consist of smelting slags from the Oiola II survey area and date from the Late Roman Empire (4th century AD). Oiola II is located 305 meters above sea level and currently 4 meters below the average level of the waters in Oiola reservoir. Between the channel of a stream, called de las Cárcavas that descends through a valley, and the bank of the river El Cuadro, appeared a terrace formed by slags, charcoal and burnt earth. This indicates an intense occupation of the soil for the transformation of the mineral into metal [31]. On this terrace three mounds were detected with remnants of slag and charcoal, and it has been proposed that these are possible iron reduction furnaces.

The Oiola IV zone is dated in the Early Middle Ages and is located in an area known as Burzako, 344 meters above sea level and 39 meters higher than Oiola II and, adjoins the municipality of

Galdames. A stream called de las Cárcavas runs bellow this area and flows into the River El Cuadro mentioned above, which in turn feeds the current Oiola reservoir with waters. The settlement has a spatial extension of about 1,000 m^2 corresponding to a rectangle approximately 47 x 30 meters in size. Two of the sides are limited by the de las Cárcavas stream and another stream that descends from Grameran Mountain. During the different campaigns, slag remains were found on the surface of a large embankment and the structure of a smelting furnace [31].

The transformation of the landscape due to iron mining until the 20th century and the subsequent abandonment of mining work have left the archaeological site of Oiola currently submerged under a lake.

4. Materials and Methods

4.1. Slag sampling and processing

The studied samples were 31 ferrous smelting slags stored in Bilbao Arkeologi Museoa (Bilbao, Spain). Ten of these samples correspond to Roman slags from the Oiola II zone. The remaining 21 slags belong to the Oiola IV area and date from the Middle Ages. The slag samples were typically pieces several centimeters in size, < 8 × 5 × 4 cm, and were hardly weathered on their surface.

The macroscopic examination of the selected ferrous material samples was able to discriminate different sample groups according to macroscopic features. The slags were further studied by microscopic and compositional analyses.

Slag textural and geochemical analyses were performed by optical microscopy, Scanning electron microscopy with energy dispersive X-ray spectroscopy (SEM-EDX), X-ray diffraction (XRD) and Thermo-gravimetric analysis (TGA) techniques. For this purpose, each slag was divided in two parts: one for textural observations by means of a polished thin section and the second was crushed and pulverized for mineral studies.

4.2. Optical microscopy

The mineralogical and textural characterization of slags were observed in thin-sections by light polarized microscopy using a petrographic polarizing Nikon Eclipse LV100POL microscope equipped with an Olympus DS F-11digital camera. The microscope observations were performed using both transmitted and reflected light modes.

4.3. X-ray powder diffraction

The mineralogical assemblage of slags was determined by an MDP Phillips (X'Pert Pro model) diffractometer for polycrystalline samples. The diffractometer is equipped with two Theta 2Theta goniometers operating independently sharing a single source of X-rays and equipped with secondary monochromator. One goniometer is used for high temperature measurements (Anton Paar HTK16 camera). The second goniometer operates with an automatic 15-position charger. The operating conditions were 40 kV and 20 mA, suitable for routine measurements of powder samples. Phase identification was made by using the quartz present in the samples as an internal standard in the random orientation of the powdered material.

Powder X-ray Thermodiffraction (TDX) was performed to observe phase transitions in order to simulate the smelting process. XRD data were collected on a Bruker D8 Advance diffractometer operating at 30 kV and 20 mA, equipped with a Cu tube (λ = 1.5418 Å), a Vantec-1 PSD detector, and an Anton Parr HTK2000 high-temperature furnace. The powder patterns were recorded in 2 steps of 0.033° in the $20 \leq 2 \leq 70$ range, counting for 3s per step (total time for each temperature 1:24 h). Data sets were recorded from 30 to 1205 each 25 °C at 0.166 °C s^{-1} heating rate.

A systematic procedure for phase identification was by ordering the d-spacings of the most intense peaks. Files of d-spacings for hundreds of thousands of inorganic compounds are available from the International Centre for Diffraction Data as the Powder Diffraction File (PDF) integrated in the software of the instrumentation.

4.4. Scanning electron microscopy with energy dispersive X-ray spectroscopy

Sample mineralogical and textural characterization were performed using a JEOL JSM 6400 scanning electron microscope (SEM) operating with an INCA EDX detector X-sight Series Si (Li) pentaFET Oxford. Samples were carbon-coated to eliminate charging effects. Microtextural observations and elemental analysis were performed on polished thin sections. Qualitative microanalysis was carried out using the ZAF method, which is based on the correction of the matrix effect in multielemental analysis that takes place in the simultaneous determination of the concentration of each element present in a multi-element material. This method provides X-ray intensity correction, absorption correction, and the fluorescence correction produced by the atomic number effect of each element, by the composition and depth of electron penetration, and by the secondary fluorescence respectively. The counting time for punctual analyses was 60 s. Concentrations were calculated by stoichiometry from elements generated by ZAF software.

4.5. Raman microspectroscopy

Raman spectra were performed with a Renishaw inVia Raman spectrometer coupled with a Leica DMLM microscope using three objectives (5×, 20×, and 50×), resulting in a spot of 1–2 μm. A+ laser with a wavelength of 514 nm and 785 nm (NIR) with a holographic net of 1800 lines/mm grating was used for the analyses. Lasers have a nominal power at the source of 50mW and 400mW, and the maximum powers at the sample are 20mW and 500mW, respectively. Spectra were recorded between 1000-100 cm^{-1} with a 1 cm^{-1} resolution and a good signal-noise ratio. The system is equipped with a CCD detector cooled down by a Peltier cooling system. Raman spectra were collected with Renishaw's WiRE™ 2.0 software and the peak search algorithm embedded in the software was used to determine the wavenumber for each Raman mode.

4.6. Thermo-gravimetric analysis (TGA)

Thermogravimetric analysis (TGA) was performed in a TA SDT 2960 TG-DSC simultaneous instrument (TA Instruments, New Castle, DE, USA). 5mg of the sample were heated at 2 °C min^{-1} from room temperature to 1200 °C. Thermogravimetry is a technique used to define the change in the mass of a sample caused by an imposed temperature regime, or a technique used to measure the mass of the sample in the function of temperature. The measurement results in a thermogravimetric curve (TG curve) that shows the dependence of the sample mass on time/temperature and a DSC curve where the change in the difference in the heat flow rate to the sample and to the reference material is measured as a function of temperature. Thus, TGA analysis is able to establish temperature conditions during the process of iron reduction in ancient bloomery furnaces. Therefore, in order to reproduce the furnace conditions, both inert and oxidizing atmospheres were employed in TGA analyses.

The XRD, SEM-EDX and Raman microspectroscopy analyses were performed in the Materials and Surface Unit and in the Raman-LASPEA laboratory of the Advanced Research Facilities (SGIker) in the Basque Country University (UPV/EHU). TGA analyses were carried out in the Inorganic Chemistry Department in the Basque Country University (UPV/EHU).

5. Results and Discussion

All the analyzed samples correspond to smelting slags; most are tap-slags and a few furnace-bottom slags (plano-convex shape), with variable magnetism and porosity, and rippled smooth black surfaces. Nevertheless, all slags from the Roman Period correspond to tap-slags, except one of them that is cinder type (Table 1).

Table 1. Studied smelting slags indicating the age of samples and macroscopic features.

	Site	Period	Age	Sample	Slag type	Slag features
⊐	OIOLA IV	Early Middle Ages	5th to 10th	OI-26-2	Tap-slags	Strong

Preprints (www.preprints.org) | NOT PEER-REVIEWED | Posted: 11 January 2020 doi:10.20944/preprints202001.0111.v1

Peer-reviewed version available at Minerals 2020, 10, 321; doi:10.3390/min10040321

			centuries AD	OI-32 OI-33-44E OI-33-45E		magnetism and porosity
Group 2	OIOLA IV	Early Middle Ages	5th to 10th centuries AD	OI-18 OI-22-13E OI-22-18E OI-22-51E	Plano-convex Tap-slags	Medium magnetism and porosity
Group 3	OIOLA IV	Early Middle Ages	5th to 10th centuries AD	OI-19 OI-20 OI-21 OI-22-16E OI-22-23E OI-23-22E OI-25-43E OI-25-50E OI-26-1 OI-27 OI-28 OI-31 OI-27-57E	Tap-slags Plano-convex	Low / absence of magnetism and porosity
	OIOLA II	Late Roman Period	4th century AD	OI-II-02 OI-II-03 OI-II-04 OI-II-05 OI-II-06 OI-II-07 OI-II-08 OI-II-09 OI-II-10 OI-II-12	Tap-slags Cinder slags	Strong magnetism and low porosity

To the naked eye, within the samples from Oiola IV (Middle Age period), three groups of slags were established according to the pore amount and grade of magnetism, while Roman slags from Oiola II, conversely, constitute a single group. The first group of smelting slags from Oiola IV presents strong magnetism and high porosity (Fig. 2a). The second group of slags shows a medium degree of magnetism and porosity (Fig. 2b). Finally, the third group shows low/absence of magnetism and porosity (Fig. 2c). All Roman slags show strong magnetism but low porosity. Thus, macroscopic characteristics only establish a clear relationship between the degree of magnetism and porosity in slags from Oiola IV, but not whether the slags correspond to bottom or tap-slags.

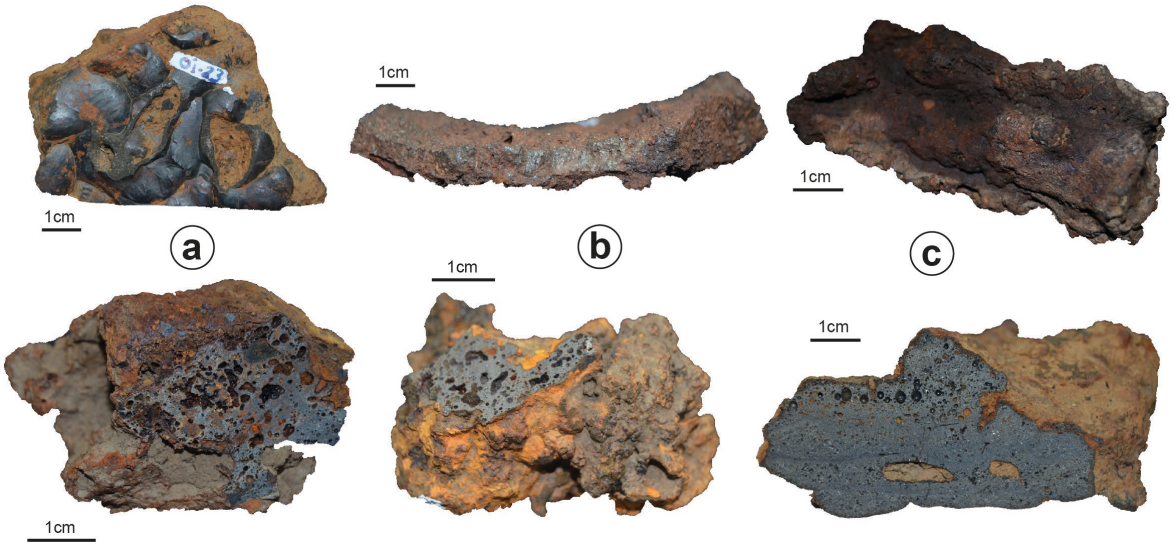

Figure 2. General aspect of the studied smelting slags in cut section. (**a**) Slags from Oiola IV with strong magnetism; (**b**) slags from Oiola IV with medium grade of magnetism; (**c**) Slags with low/absence of magnetism from Oiola IV.

Optical microscopy allows the observation of the textural and mineralogical characteristics of smelting slags. The optical micrographs show the typical structure of the investigated samples, formed mainly by olivine and wuestite and a low amount of quartz. Texturally, most olivines show skeletal morphologies although massive olivines can also be found (Fig. 3a, 3b). Olivines can be easily distinguished by optical microscopy in transmitted light mode because of the high birefringence and lack of cleavage. Wuestite displays a dendritic morphology and is embedded and intergrown within the olivines (Fig. 3c). In reflected light mode, magnetite can also be distinguished since it forms euhedral crystals and sometimes cruciform-skeletal crystals indicating a rapid crystallization [32] (Fig. 3b). Textural features and the lighter bright grey color of magnetite discriminate reasonably well from wuestite by reflected light [33]. Moreover, in samples from the Roman Period occasionally sub-rounded small white particles are present corresponding to metallic iron. These iron particles are scarce, in comparison with other iron oxides, but are absent in Medieval slags from Oiola IV.

Slags showing low magnetism display some white lines evidencing a layered structure. These lines are thin skins that indicate the separation of the individual slag flows coming out of the furnace (Fig. 3d). This microstructure reflects the solidification of subsequent flows of slag resulting in a layered structure. Elongated olivine crystallizes perpendicular to the white skins, which means that the lower flow was already cooled before the following flow arrived. This structure is well known from geological lava flows and tap-slags as spinifex texture [34]. White lines in smelting slags are explained as thin skins of magnetite formed when the surface of the slag flow oxidizes in contact with air [34,35].

Phase associations identified by XRD are summarized in Table 2. The determined mineralogy is in accordance with the petrographic observations. Samples from Oiola IV (Early Middle Ages) are mainly constituted by olivine and wuestite, while the wuestite content in the Roman slags from Oiola II is variable. Magnetite is present in slags with high/moderate degree of magnetism. Quartz is also identified in most of the smelting slags in variable amounts.

Preprints (www.preprints.org) | NOT PEER-REVIEWED | Posted: 11 January 2020 doi:10.20944/preprints202001.0111.v1

Peer-reviewed version available at Minerals 2020, 10, 321; doi:10.3390/min10040321

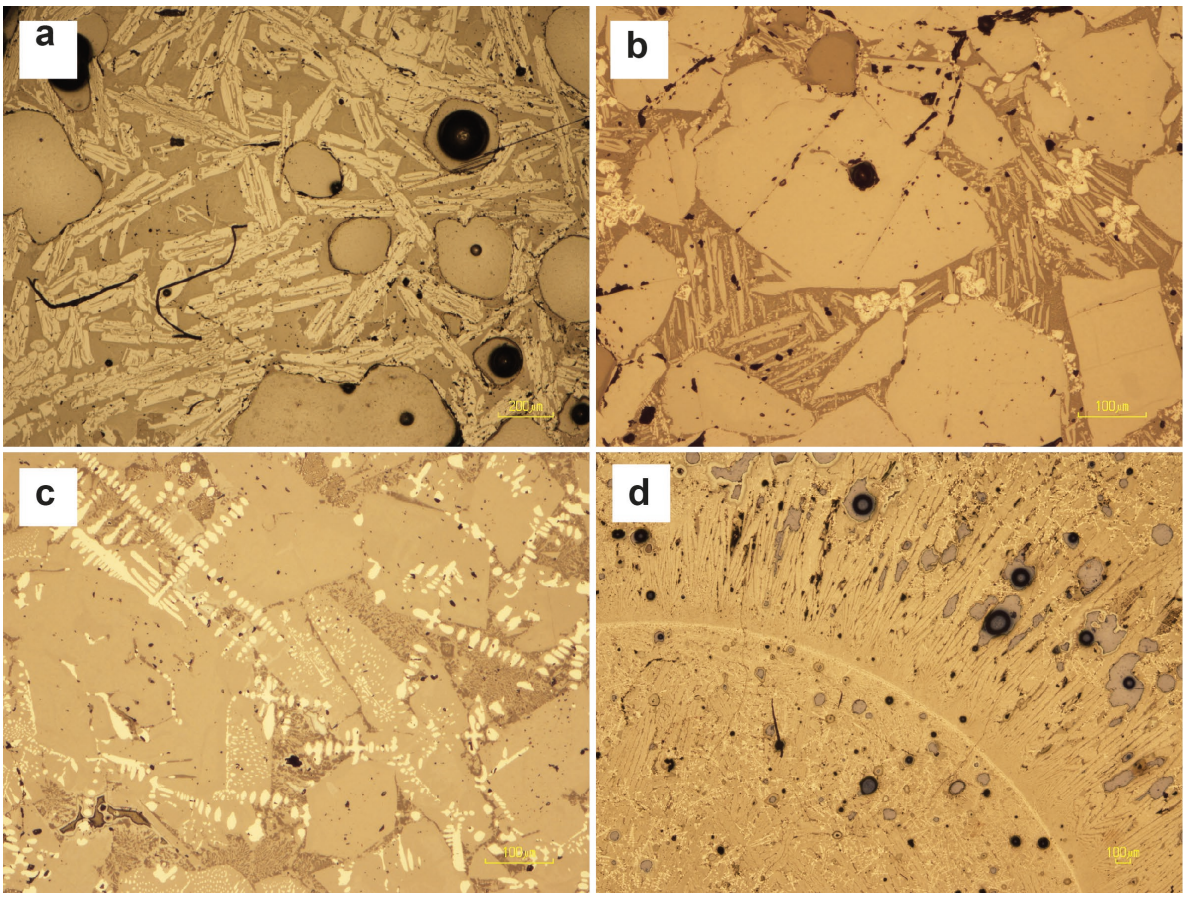

Figure 3. Photomicrographs showing microtextures of polished samples. (**a**) skeletal olivines. (**b**) massive olivines and cruciform-skeletal crystals of magnetite. (**c**) dendritic Wuestite intergrowing within the olivines. (**d**) white lines of magnetite indicating different slag flows.

Raman spectroscopy was used to characterize the mineralogy of white skins. Bands at 300 cm^{-1}, 544 cm^{-1} and 672 cm^{-1} are attributed to magnetite [36] (Fig. 4). The identification of magnetite in the white lines is in accordance with the published literature [34,35]. Additionally, two intense bands in the region of 700 and 1100 cm^{-1} are attributed to Fe-rich olivine corresponding to fayalite member [37-39].

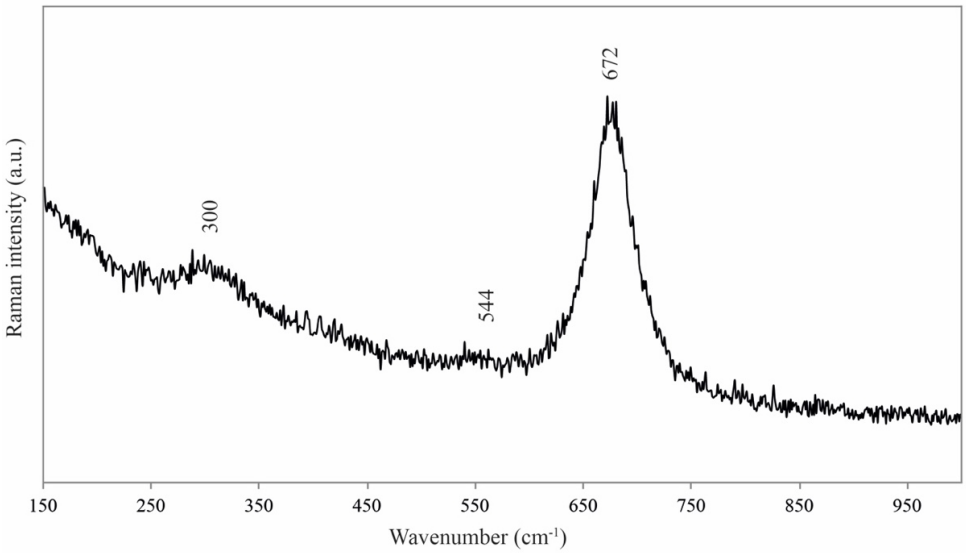

Figure 4. Raman spectra of the white skins of magnetite.

Peer-reviewed version available at Minerals 2020, 10, 321; doi:10.3390/min10040321

Table 2. XRD mineralogical composition of studied samples.

Sample	Period	Mineralogy			
		Quartz	Magnetite	Olivine	Wuestite
OI-26-2	Early Middle Ages	*	**	***	**
OI-32		**	*	**	*
OI-33-44E		*	**	***	**
OI-33-45E		***	*	*	*
OI-18			*	***	**
OI-22-13E			*	***	**
OI-22-18E		*	*	***	*
OI-22-51E		**		***	
OI-19		*		***	**
OI-20		*		***	**
OI-21				***	**
OI-22-16E				***	**
OI-22-23E		*		***	
OI-23-22E		**		***	**
OI-25-43E		*	*	***	**
OI-25-50E				***	**
OI-26-1				***	**
OI-27		*		***	**
OI-27-57E				***	*
OI-28		**		***	**
OI-31		*		***	*
OI-II-02	Late Roman Period	*	*	***	**
OI-II-03		*	**	***	
OI-II-04		**	**	***	
OI-II-05			**	***	**
OI-II-06		*	*	***	**
OI-II-07		*	*	***	**
OI-II-08		*	***	**	**
OI-II-09			**	***	**
OI-II-10			*	***	**
OI-II-12		*	**	***	**

*** very abundant, ** abundant, * present

SEM-EDS analyses reinforce the mineralogical assemblage and the structures observed in the microscopic analysis. Skeletal and polyhedral olivines show light-grey colors, while dendritic wuestite and cruciform magnetite are white (Fig. 5a). Magnetite white skins and the spinifex texture are also well observed at this scale (Fig. 5b). However, in slags with low magnetism, cruciform morphologies were also found but EDS analyses showed the presence of aluminum indicative of a mineral phase of the spinel group, corresponding to hercynite (Fig. 5c, 5d). SEM-EDS analysis shows that all of the slag samples contain a small amount of glassy phase distributed in very reduced areas, but in high magnification dendritic wuestite is present (Fig. 5c).

Peer-reviewed version available at Minerals 2020, 10, 321; doi:10.3390/min10040321

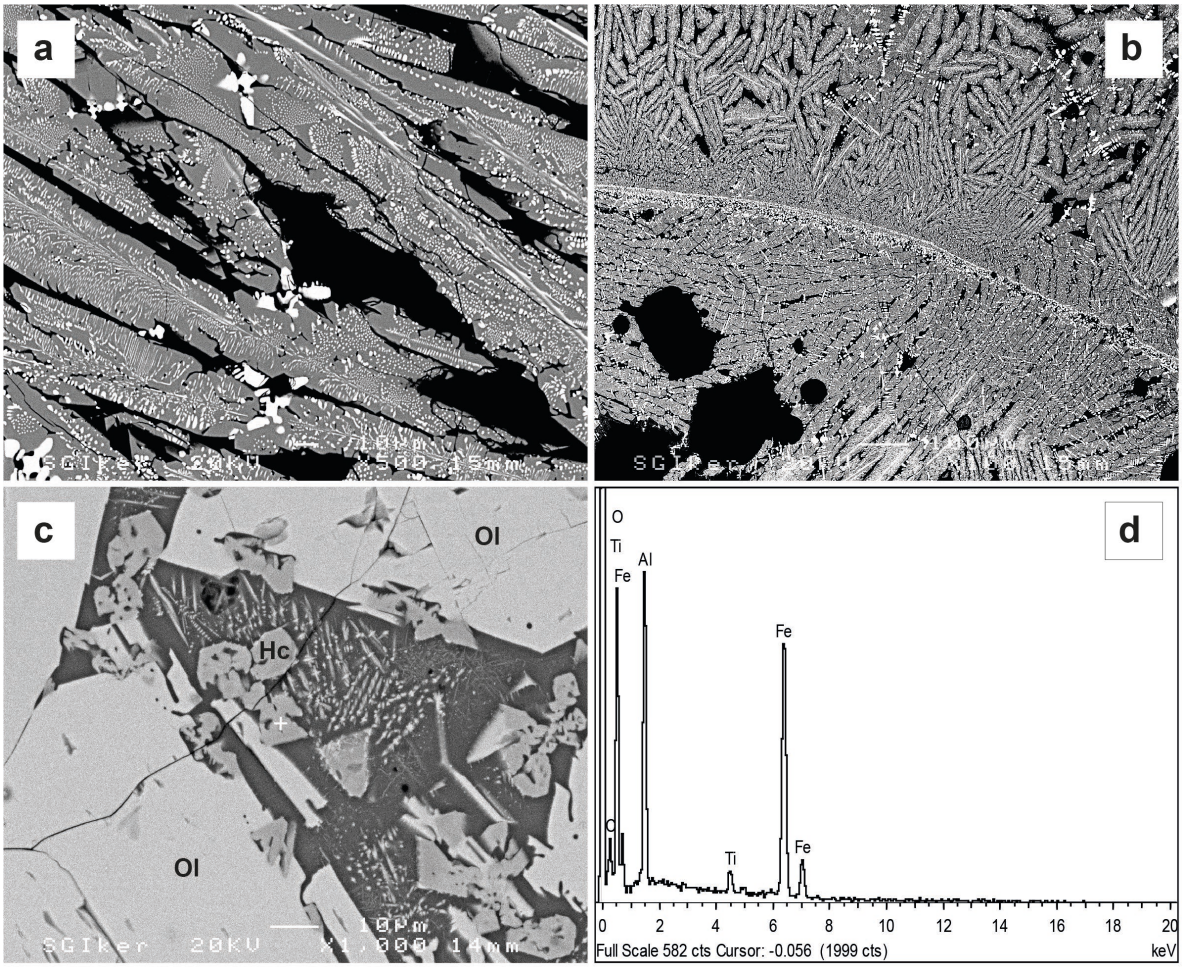

Figure 5. SEM-BSE images. (**a**) skeletal and polyhedral olivines (light-grey colors), dendritic wuestite and cruciform magnetite (white colors). (**b**) magnetite white skins and the spinifex olivines. (**c**) polyhedral olivines (light-grey colors) and euhedral-cruciform hercynite (grey colors). d) EDS spectra of hercynite from + point in the previous image.

Microchemical composition of the matrix can be used to determinate some technological parameters of the smelting process. Unfortunately, the glassy areas were not big enough to allow quantitative analysis. In addition, in high magnification skeletal wuestite crystals appear within some areas leading to uncertain measurements.

Due to the unknown chemical composition of the glassy matrix, temperature-dependent powder X-ray diffraction was performed to determine the pyrometallurgical conditions prevailing in antiquity. An ore sample was heated in a high temperature chamber in environmental conditions to observe phase transitions occurring at different temperatures. The ore sample consists of goethite and a minor amount of quartz. Figure 6 shows the mapping of the TDX. During heating only a phase transition of goethite towards hematite can be observed at 300 °C. Besides, at 870 °C the crystallization of trydimite can be observed. The absence of wuestite and/or magnetite indicates the influence of the oxidizing conditions used in the simulation. Also the absence of olivine can be related to the low amount of quartz.

The transition temperatures obtained in environmental conditions simulated by X-ray diffraction differ from measurements performed under reducing conditions. To characterize smelting conditions used in ancient ironmaking in Oiola, Thermo-Gravimetric Analysis (TGA) was carried out in both inert and environmental atmospheres with simultaneous recording of the loss of weight of the sample while temperature rises at a uniform rate. Nevertheless, the net weight loss and the kinetic parameters obtained are based on simplifying assumptions which do not necessary

Peer-reviewed version available at Minerals 2020, 10, 321; doi:10.3390/min10040321

correspond to the complex chemical reactions occurring during the transformation of iron ores into metal.

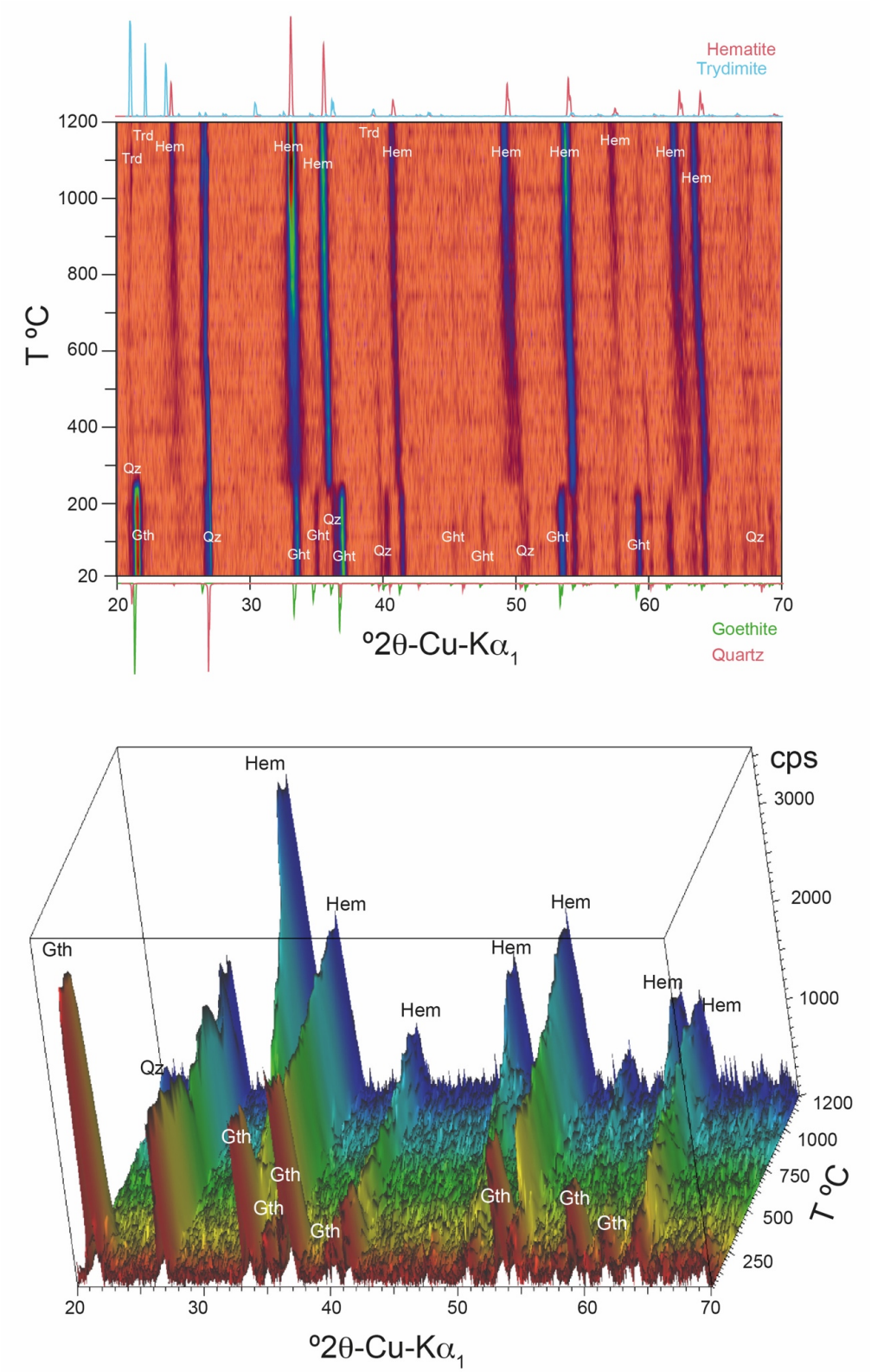

Figure 6. Thermodiffraction patterns for iron ore heated between 30-1205 ºC and 2θ range from 20 to 70 º as stacked patterns showing phase transition at different temperatures. Upper figure: stacking of 1D diffractograms; lower figure: stacking of 3D diffractograms.

Peer-reviewed version available at Minerals 2020, 10, 321; doi:10.3390/min10040321

The results of thermal analysis of goethite ore powder is shown in Figure 7. Upon heating, the DSC/TG profiles in both atmospheres show an endothermic peak at around 300 °C with an associated weight loss of 10.7% due to the dehydroxylation of goethite. At this temperature the goethite (FeOOH) transforms into hematite (Fe_2O_3) (Fig. 7a). The relatively low weight loss (< 1% of weight) observed between 530 °C to 600 °C related to the decomposition of clays could not be identified [40-42]. In the DSC curve of environmental conditions, a second stage was identified corresponding to the reduction of iron ore between 650 °C and 960 °C related to the transformation of hematite into magnetite and magnetite into Fe respectively [41]. The endothermic peak found at 1140 °C was attributed to the melting temperature. Conversely, in inert atmosphere the iron ore reduction was not observed because it may be found at temperatures higher than 1200 °C (Fig. 7b). Thermogravimetic and heat curves for goethite ore powder in a rate of 70/40% with quartz are also shown in Figure 7b. Addition of quartz as flux material decreases the reduction temperatures of iron ore reduction stages and the melting point occurs at 890 °C. The addition of flux elements decreases the melting temperature by around 250 °C.

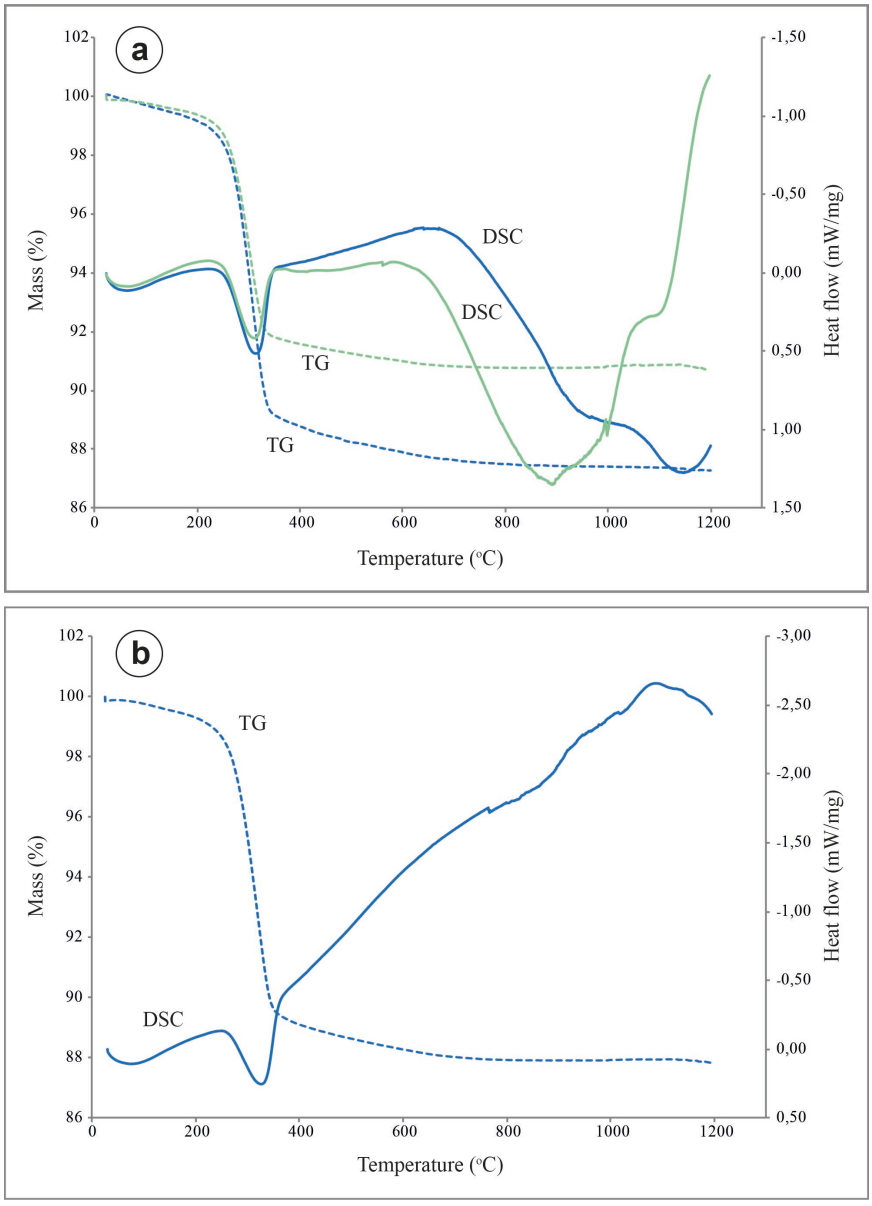

Figure 7. Thermogravimetric profiles of iron ore. (**a**) DSC/TG curves in environmental atmosphere of iron ore and iron ore with quartz flux. (**b**) DSC/TG curves in inert atmosphere.

Mineralogical and textural features of slags together with temperature-dependent reactions can be used to explore the pyrometallurgical conditions in ironmaking from the Roman Age to the Early Middle Ages. The morphology and crystal size distribution indicate different smelting temperatures. Dendritic wuestite indicates a fast cooling of tap-slags outside the furnace (Figs. 3c, 5a). Fast cooling also resulted in skeletal olivines whereas massive olivines indicate slower cooling rates (Figs. 3a, 3b, 5a, 5b). Skeletal and dendritic morphologies suggest temperature cooling rates around 100 °C [43]. Mineral assemblage of slags is also able to estimate the furnace operating conditions. The presence of magnetite can be explained as an oxidation process during the iron smelting. In fact, Early Medieval slags with strong magnetism show high porosity and dispersed cruciform magnetite. The air trapped in the porous system yielded the wuestite oxidation to magnetite. Nevertheless, Roman slags with strong magnetism show low porosity, indicating an inefficient smelting process and suggesting an excess of air supply into the furnace [44]. Unlike highly magnetic slags, magnetite skins present in slags with low magnetism suggest an oxidation of the surface of subsequent slag flows coming out of the furnace.

Spinel-like phases (hercynite) detected in the Oiola smelting slags indicate the use of an aluminum-bearing ore composed mainly of goethite and quartz and clay minerals. The presence of clay minerals indicates a total use of iron bog ores including the ferric upper supergenic horizon. Besides, differences in magnetite content between Roman and Medieval smelting slags suggest an improvement in the control of reduction conditions in bloomery furnaces.

Dendritic wuestite and the assemblage of olivine and wuestite in smelting slags suggest furnace temperatures lower than 1200 °C. Nevertheless, the lowest melting temperature of iron is 1560 °C; higher than the bloomer furnace's capability [7,45]. The addition of fluxes like quartz allows the iron melting temperature to be decreased to 1000 °C and 1100 °C [12]. In fact, the results of TGA analyses with the addition of quartz as a flux show a melting temperature decrease from 1140 °C to 890 °C. Even though the iron ore at Oiola is a mixture of goethite and quartz, the lack of olivine and wuestite in the TDX analyses indicates a small amount of quartz in the ore to behave as a flux and decrease the melting temperature.

6. Conclusions

Evidence of bloomery smelting wastes found in Oiola Archaeological site indicates that iron mining in the mining complex of La Arboleda (Biscay) during the 19th - 20th centuries, goes back to the Roman Period. The morphological features and spinifex textures indicate that most slags from Oiola correspond to tap-slags. Smelting slags from Oiola also provide information about bloomery furnace temperatures and cooling rates. Mineral textures corresponding to skeletal and dendritic morphologies of olivine and wuestite suggest rapid cooling rates. The presence of magnetite indicates poor control of the ventilation system in the furnace due to a large oxygen supply, reflected by the variable porosity of slags, leading to wuestite oxidation. Besides, samples showing hercynite mineral confirm the use of bog iron ore composed mainly of goethite, quartz and clay minerals as the raw material used in the ironmaking. Mineral assemblages also allow furnace temperature and operating conditions to be determined. The results show a transformation of goethite to hematite at around 300°C and a reduction of the iron ore between 650 °C and 960 °C. Moreover, the addition of quartz as a flux resulted in a melting temperature decrease of the ore of around 200 °C. The multianalytical approach to bloomery slags provides a better understanding of iron processing at Oiola iron smelting site. The comparison of the mineralogical assemblage and textural features of smelting slags from the Late Roman Period and the Early Middle Ages suggests changes in the pyrometallurgical process.

Acknowledgments: This study was supported by the IT1193-13 project of the Basque Country Government. H.P. would like to thank the PRE-2019-2-0138 PhD research grant of the Basque Country Government and the SGIker service at the University of the Basque Country. The authors would also like to thank Peter Smith for language assistance.

Peer-reviewed version available at Minerals 2020, 10, 321; doi:10.3390/min10040321

References

1. Pleiner, R. Iron in archaeology: The European bloomery smelters. Archeologický Ústav Aveř, 2000.
2. Serneels, V.; Perret, S. Quantification of smithing activities based on the investigation of slag and other material remains. In Archaeometallurgy in Europe-Proceedings of the International Conference. Milan, Italy: Associazione Italiana di Metallurgia **2003**, 469-478.
3. Coustures, M. P.; Béziat, D.; Tollon, F.; Domergue, C.; Long, L.; Rebiscoul, A. The use of trace element analysis of entrapped slag inclusions to establish ore–bar iron links: examples from two Gallo-Roman iron-making sites in France (Les Martys, Montagne Noire, and Les Ferrys, Loiret). Archaeometry **2003**, 45(4), 599-613.
4. Selskienė, A. Examination of smelting and smithing slags formed in bloomery iron-making process. Chemija **2007**, 18(2).
5. Senn, M.; Gfeller, U.; Guénette-Beck, B.; Lienemann, P.; Ulrich, A. Tools to qualify experiments with bloomery furnaces. Archaeometry **2010**, 52(1), 131-145.
6. Charlton, M. F.; Blakelock, E.; Martinón-Torres, M.; Young, T. Investigating the production provenance of iron artifacts with multivariate methods. Journal of archaeological Science **2012**, 39(7), 2280-2293.
7. Charlton, M. F., Crew, P.; Rehren, T.; Shennan, S. J. Explaining the evolution of ironmaking recipes–An example from northwest Wales. Journal of Anthropological Archaeology **2010**, 29 (3), 352-367.
8. Parreño, C. M.; Martín, A. M.; Ferrer Eres, M. Á. Iron, Fuel and Slags: reconstructing the Ironworking Process in Iberian Iron Age (Valencian Region). Pyrenae **2009**, 40(2), 105-127.
9. Tylecote, R. F. Furnaces, crucibles and slags, in the coming of the age of iron (eds. T. A. Wertime and J.D. Muhly), Yale University Press, New Haven, CT **1980**, 183-226.
10. Buchwald, V. F.; Wivel, H. Slag analysis as a method for the characterization and provenancing of ancient iron objects. Materials characterization **1998**, 40(2), 73-96.
11. Bayley, J.; Dughworth, D.; Paynter, S. Centre for Archaeology guidelines: archaeometallurgy, English Heritage, London, 2001.
12. Ros-Latienda, L.; Fernández Carrasquilla, J. Caracterización de escorias metalúrgicas procedentes de yacimientos arqueológicos de Navarra (Siglos II aC-IV dC). Revista de Metalurgia **2013**, 49(6).
13. Eekelers, K.; Degryse, P.; Muchez, P. Petrographic investigation of smithing slag of the Hellenistic to Byzantine city of Sagalassos (SW-Turkey). American Mineralogist **2016**, 101(5), 1072-1083.
14. Blakelock, E.; Martinon-Torres, M.; Veldhuijzen, H. A.; Young, T. Slag inclusions in iron objects and the quest for provenance: an experiment and a case study. Journal of Archaeological Science **2009**, 36(8), 1745-1757.
15. Cleere, H. Some operating parameters for Roman ironworks. Bulletin of the Institute of Archaeology **1976**, 13, 233-246.
16. Crew, P. The influence of clay and charcoal ash on bloomery slags. In Il Ferro nelle Alpi, giacimenti miniere e metallurgia dall'antichità al XVI secolo, Atti del Convegno **2000**, 38-48.
17. Paynter, S. Regional variations in bloomery smelting slag of the Iron Age and Romano-British periods. Archaeometry **2006**, 48(2), 271-292.
18. Gordon, R. B. Process deduced from ironmaking wastes and artefacts. Journal of Archaeological Science **1997**, 24(1), 9-18.
19. Benvenuti, M.; Mascaro, I.; Costagliola, P.; Tanelli, G.; Romualdi, A. Iron, copper and tin at Baratti, Populonia: smelting processes and metal provenances. Historical metallurgy **2000**, 34(2), 67-76.
20. Török, B.; Gallina, Z.; Kovacs, A.; Kristaly, F. Early medieval iron bloomery centre at Zamárdi (Hungary) Complex archaeometrical examinations of the slags. Archeologické Rozhledy **2018**, 70(3).
21. Tylecote, R. F.; Austin, J. N.; Wraith, A. B. The mechanism of the bloomery process in shaft furnaces. Journal of the Iron and Steel Institute **1971**, 342-363.
22. Kaczorek, D.; Sommer, M. Micromorphology, chemistry, and mineralogy of bog iron ores from Poland. Catena **2003**, 54, 393-402.
23. Kaczorek, D.; Sommer, M.; Andruschkewitsch, I.; Oktaba, L.; Czerwinski, Z.; Stahr, K. A comparative micromorphological and chemical study of "Raseneisenstein" (bog iron ore) and "Ortstein". Geoderma **2004**, 121, 83-94.
24. Banning, A. Bog iron ores and their potential role in arsenic dynamics: an overview and a "Paleo Example". Engineering in Life Sciences **2008**, 8, 641-649.

25. Thelemann, H.; Bebermeier, W.; Hoelzmann, P.; Lehnhardt, E. Bog iron ore as a resource for prehistoric iron production in Central Europe - A case study of the Widawa catchment area in eastern Silesia, Poland. Catena **2017**, 149, 474–490.
26. Kaczorek, D.; Brümmer, G.; Sommer,M. Content and binding forms of heavy metals. Aluminium and phosphorus in bog iron ores from Poland. J. Environ. Qual. **2005**, 38, 1109–1119.
27. García-Mondéjar, J.; Fernández-Mendiola, P.A.; Agirrezabala, L.M.; Aranburu, A.; López-Horgue, M.A.; Iriarte, E.; Martínez de Rituerto, S. El Aptiense-Albiense de la Cuenca Vasco-Cantábrica. La Cordillera **2004**, 291-296.
28. Gil Crespo, P.P. Las mineralizaciones de hierro en el anticlinal de Bilbao: mineralogía, geoquímica y metalogenia. Tesis Doctoral, inéd, Univ. País Vasco, 1991.
29. Rzepa, G.; Bajda, T.; Ratajczak, T. Utilization of bog iron ores as sorbents of heavy metals. Journal of Hazardous Materials **2009**, 162, 1007–1013.
30. Beukes, N. J.; Gutzmer, J.; Mukhopadhyay, J. The geology and genesis of high-grade hematite iron ore deposits. Applied Earth Science **2003**, 112, 18-25.
31. Pereda García, I. La metalurgia prehidráulica del hierro en Bizkaia: el caso de los alrededores del pantano de Oiola (Trapagarán, Bizkaia). Kobie (serie paleoantropología) **1992**, 109-122.
32. Ixer, R. A. Atlas of opaque and ore minerals in their associations. Osprey Books, 1990.
33. Ramdohr, P. The ore minerals and their intergrowths. Elsevier, 2013.
34. Park, J. S.; Rehren, T. Large-scale 2nd to 3rd century AD bloomery iron smelting in Korea. Journal of Archaeological Science **2011**, 38(6), 1180-1190.
35. Ackerman, K. J.; Killick, D. J., Herbert, E. W.; Kriger, C. A study of iron smelting at Lopanzo, Equateur Province, Zaıre. Journal of Archaeological Science **1999**, 26(8), 1135-1143.
36. De Faria, D. L. A., Venâncio Silva, S.; De Oliveira, M. T. Raman microspectroscopy of some iron oxides and oxyhydroxides. Journal of Raman spectroscopy **1997**, 28(11), 873-878.
37. Chopelas, A. Single crystal Raman spectra of forsterite, fayalite, and monticellite. American Mineralogist **1991**, 76(7-8), 1101-1109.
38. Kolesov, B. A.; Geiger, C. A. A Raman spectroscopic study of Fe–Mg olivines. Physics and Chemistry of Minerals **2004**, 31(3), 142-154.
39. Mouri, T., & Enami, M. Raman spectroscopic study of olivine-group minerals. Journal of Mineralogical and Petrological Sciences **2008**, 103(2), 100-104.
40. Strezov, V., Ziolkowski, A., Evans, T.; Nelson, P. Assessment of evolution of loss on ignition matter during heating of iron ores. Journal of Thermal Analysis and Calorimetry **2009**, 100(3), 901-907.
41. Kawigraha, A., Soedarsono, J. W.; Harjanto, S. Thermogravimetric Analysis of The Reduction of Iron Ore with Hydroxyl Content. Advanced Materials Research **2013**, 774, 682-686).
42. Romero Gómez, P., González, J. C., Bustamante, A., Ruiz Conde, A.; Sánchez Soto, P. J. Estudio in-situ de la transformación térmica de limonita utilizada como pigmento procedente de Perú. Boletín de la Sociedad Española de Cerámica y Vidrio **2013**, 52, 127-131.
43. Donaldson, C. H. An experimental investigation of olivine morphology. Contributions to Mineralogy and Petrology **1976**, 57(2), 187-213.
44. Manasse, A.; Mellini, M. Chemical and textural characterisation of medieval slags from the Massa Marittima smelting sites (Tuscany, Italy). Journal of Cultural Heritage 2002, 3(3), 187-198.
45. Gómez Ramos, P. Análisis de escorias férreas: nuevas aportaciones al conocimiento de la siderurgia prerromana en España. Trabajos de prehistoria 1996, 53(2), 145-155.